10th INTERNATIONAL SCIENTIFIC CONFERENCE
ON DEFENSIVE TECHNOLOGIES
OTEH 2022
Belgrade, Serbia, 13 – 14 October 2022

MIG WELDING PROCESS ON THE MECHANICAL PROPERTIES OF BUTT WELDED JOINTS OF DISSIMILAR ALUMINUM ALLOYS 2024-T351 /6082-T6

DRAGAN MILČIĆ
Faculty of Mechanical Engineering, University of Nis, Niš, Serbia
dragan.milcic@masfak.ni.ac.rs

TOMAŽ VUHERER
University of Maribor, Faculty of Mechanical Engineering, Maribor, Slovenia
tomaz.vuherer@um.si

LJUBICA RADOVIĆ
Military Technical Institute, Belgrade, Serbia
ljubica.radovic@vti.vs.rs

MIODRAG MILČIĆ
Faculty of Mechanical Engineering, University of Nis, Niš, Serbia
miodrag.milcic@masfak.ni.ac.rs

MAJA MLADENOVIĆ
Military Technical Institute, Belgrade, Serbia
mmaja011@gmail.com

ANDREJA RADOVANOVIĆ
IMW Institut, Aleja Milanović bb, 34325 Lužnice, Kragujevac, Srbija
andreja.radovanovic@imw.rs

NENAD RADOVIĆ
Faculty of Technology and Metallurgy, University of Belgrade, Belgrade, Serbia
nenrad@tmf.bg.ac.rs

Abstract: *The aim of this work was to present the effects of the MIG welding on the mechanical properties of a butt-welded joint of dissimilar aluminum alloys 2024-T351 and AA 6082-T6. Aluminum alloy 6082 T6 is well weldable by classical fusion welding processes (MIG and TIG), while aluminum alloy 2024-T351 is almost non-weldable. For the welding of these two Al alloys, the MIG welding on 8 mm thick sheets filler material 4043A (AlSi5) and a mixture of argon and helium as a shielding gas. The assessment of the mechanical properties of the welded joint of dissimilar Al alloys was performed by Vickers hardness testing, tensile and bending tests of the welded samples. The influence of MIG welding on the microstructure of the welded joint was analyzed by light microscopy (LM) and scanning electron microscopy (SEM). It was found that the fracture of the tensile test specimen occured on the 6082-T6 aluminum alloy side. Tensile strength of the welded joint was 198 MPa, what was about 64 % of the tensile strength of the base metal, i.e. 6082-T6 alloy.*

Keywords: *Welded joints of dissimilar aluminum alloys, AA 2024-T351, AA 6082-T6, MIG welding process, Microstructure, Mechanical properties of welded joints.*

1. INTRODUCTION

Aluminum structures are often used in transport technology, in the automotive industry, in the industry of rail vehicles, in shipbuilding, in the aviation industry and even in space technologies.

Constructions of cars, trains, ships, airplanes, spacecraft, which are made of different aluminum alloys, are most often joined by classic metal inert gas (MIG) and tungsten inert gas (TIG) welding, friction stir, laser and electron beam welding. Fusion welding processes easily join materials that have good weldability. The material is well weldable if it is possible to make a welded joint without defects. The weldability of aluminum alloys is affected by a number of factors such as: oxygen affinity, high thermal expansion and thermal conductivity, high shrinkage during solidification, high solubility of hydrogen in the liquid phase, which decreases drastically during solidification. By welding aluminum alloys, mechanical

properties and corrosion resistance in HAZ are reduced, porosity, solidification and liquation cracks appear. Aluminum alloys are welded with additional material with increased content of Si or Mg [1].

Recently, leading manufacturers of welding equipment allow various modifications of MIG and TIG welding procedures, such as AC MIG with pulsing during welding with single or double pulse, or TIP TIG with automatic addition of hot wire.

If the technology of the welding procedure is not suitable, defects may appear in the area of the weld metal, which reduces the reliability of the welded structure. Weld defects such as porosity, cracks, lack of penetration or lack of fusion may appear [2].

Age-hardenable 2024 aluminum alloy belongs to the 2XXX alloy series where the main alloying element is copper. The mechanical properties of these alloys reach values similar to those of carbon steels. Such a high strength of the alloys is due to the precipitation of $CuAl_2$ particles during natural or artificial aging. As these alloys do not have good corrosion resistance, they are often coated (plated) with pure aluminum for corrosion protection. They are used for manufacturing parts in the aviation industry due to their high strength, good fatigue properties. With the addition of elements such as Mg and Li, it is possible to reduce the specific density and improve the performance of Al alloys for applications in the manufacture of parts in the aerospace industry [3]. Alloys of the 2XXX series, as a rule, have poor weldability with fusion welding (MIG, TIG), due to high crack sensitivity. Friction stir welding is mainly used for welding these alloys [4, 5].

Aluminum alloy 6082 belongs to the series of alloys age-hardenable 6XXX. Alloys where the alloying elements are silicon and magnesium. Alloys of the AI-Mg-Si system have moderate strength and good corrosion resistance, compared to other heat-treatable Al alloys. Typical of these alloys is that they have good formability and acceptable weldability.

Dissimilar aluminum alloys are being heavily used in the various fields of engineering due to its light weight and superior properties. In this paper, investigations of the mechanical behavior of the welded joint achieved by the MIG welding between dissimilar aluminum alloys 2024 T351 and 6082 T6 using the filler material S Al 4043A (AlSi5) are given.

2. MATERIALS AND METHODS

Experimental research was focused on determining the influence of the MIG welding process on the metallurgical and mechanical properties of welded joints of alloys 2024-T351 and 6082-T6.

The chemical and mechanical properties of the alloys 2024-T351 and 6082-T6 (according to standards), which are the subject of this research and joined by the MIG process, are given in Tables 1 and 2. The chemical properties of the additional material used during welding are given in Table 3.

The dimensions of the plates used for welding were 300 mm long, 125 mm wide and 8 mm thick. Welding machine was Fronius Transpuls Synergic 4000. Shielding gas was ISO 14175 – I3 –ArHe–30.

Table 1. Chemical composition of aluminum alloy 2024 T351 and 6082 T6 [6]

	Mn %	Fe %	Mg %	Si %	Cu %	Zn %	Ti %	Cr %	Al %
6082 T6	0.4-1.0	0- 0.5	0.6-1.2	0.7-1.3	0-0.1	0-0.2	0-0.1	0-0.25	Balance
2024 T351	0.65	0.17	1.56	0.046	4.7	0.11	0.032	-	Balance

Table 2. Mechanical properties of aluminum alloy 2024 T351 and 6082 T6 [6]

	Yield strength min R_{eh} |(Mpa)	Ultimate tensile strength min R_m (Mpa)	Elongation at Break min A(%)	Hardness HV
2024 T351	310	425	10	137
6082 T6	260	310	10	95

Table 3. Chemical composition of the filler material of wire EN ISO 18273 S Al 4043A (AlSi5), mas. %

Mn %	Fe	Mg	Si	Cu	Zn	Ti	Be	Al
<0,15	<0,6	<0,2	4,5-5,5	<0,3	<0,1	<0,15	<0,0003	Balance

Table 4. Welding parameters for the MIG butt weld welding process for the material EN AW 2024-T351/EN AW 6082-T6

Run	Welding Process EN ISO 4063	Current I (A)	Voltage U (V)	Wire Feed Speed (m/min)	Welding Speed v (mm/s)	Heat input H=I·U·□/v (J/mm)
1	131	150	21	6,2	7	360
2	131	160	22	6,5	11,5	245
3	131	160	22	6,5	7,7	366

Vickers hardness was measured on a Willson VH1150 hardness tester. Tensile properties were determined at room temperature using a Shimadzu AG-X 300 kN tensile tester. Test specimens defined by the ASTM E8M standard obtained from welded samples perpendicular to the welded joint were used [7]. Specimens were cut from the welded samples using the water jet cutting process.

The bending tests were carried out on four specimens—in two the tensiled side was the face of the weld and in two the tensiled side was the root of the weld. The test was performed at room temperature using the three-point bending method.

A Leica Q500MC optical microscope (LM) was used to analyze the microstructure of the welded joint. The microstructure was examined on the cross-section of the samples after the usual metallographic preparation and etching in Keller's reagent. The tests were also carried out using the scanning electron microscope JOEL JSM-6610LV (SEM).

3. RESULTS

Figure 1 shows face side of a welded joint. Welded joint made with a backing material.

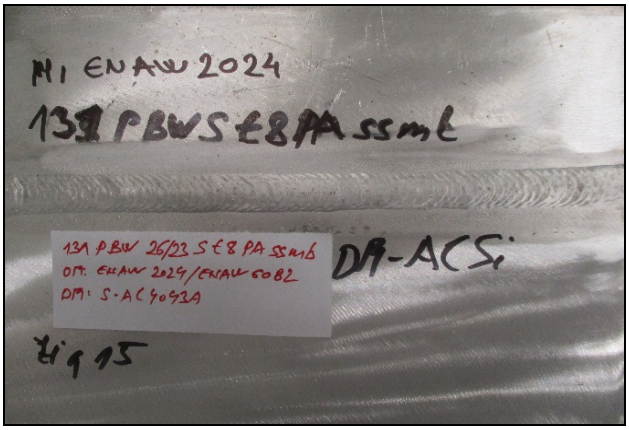

Figure 1. Face side of the welded joint.

3.1. Destructive Tests

3.1.1. Static Tensile Test

Figure 2 shows the specimen after breaking.

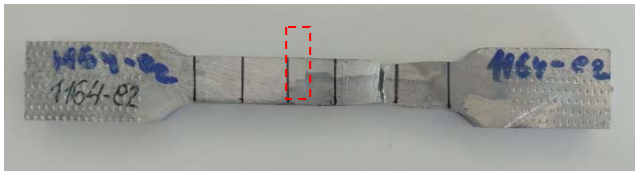

Figure 2. Specimen after a static tensile test.

Stress-strain curves is shown in Figure 3, and results are summarized in Table 5. The fracture was ductile and occurred in the 6082 base material (BM).

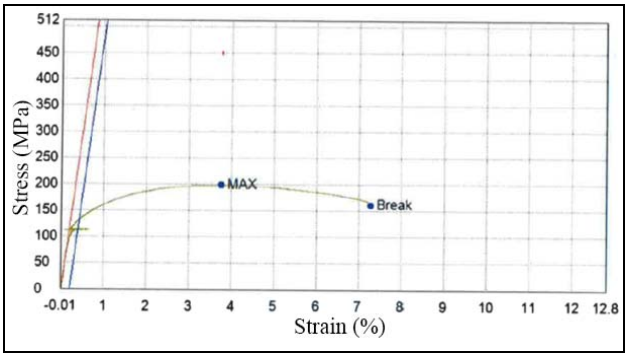

Figure 3. Stress-strain diagram.

Table 5. Tensile test results of welded joints

Cross-section area (mm^2)	Yield strength R_{eh} (MPa)	Ultimate tensile strength R_m MPa)	Elongation at break A (%)	Place of fracture
80	113	198	7.3	BM 6082 T6

3.1.2. Bending Test

Root and face bending tests are given in Figure 4 and 5. The aim of this test was to investigate the plastic properties of the welded joint.

Figure 4. Root bend test.

The results shown small bending angle until the appearance of a crack in both root and face bend test. However, weld joint showed more ability to withstand deformation under face bend test.

Hardness measurements were made as shown in Figures 6 and 7.

The hardness of the weld metal, measured near the weld face and near the weld root, is about 80 HV, while hardness of base metals are about 90 HV and 150 HV for 6082-T6 and 2024-T351. The hardness of HAZ towards 6082-T6 and 2024-T351 is about 60 HV and 120 HV, respectively.

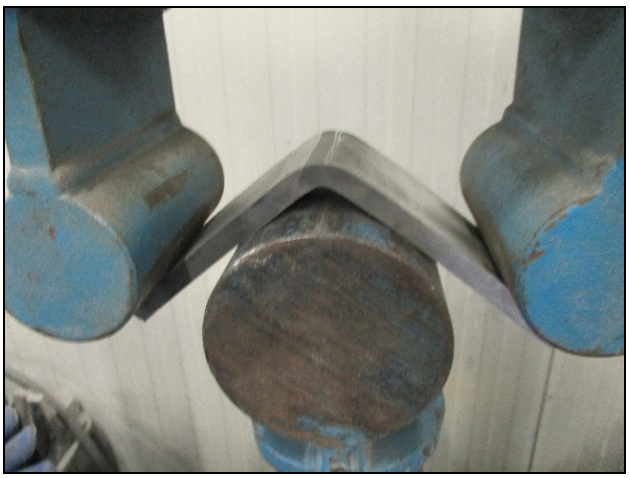

Figure 5. Face bend test.

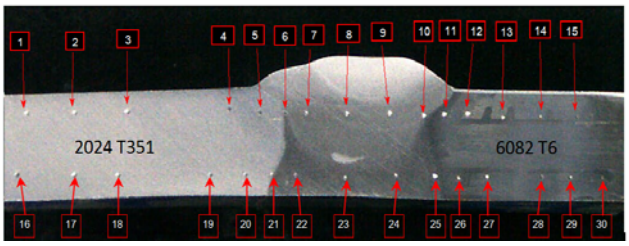

Figure 6. Hardness measurement of the joint.

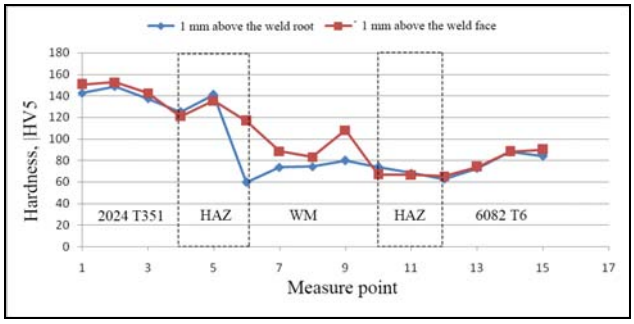

Figure 7. Hardness distribution of the joint.

3.1.3. Macro- and Microscopic Examinations

Figure 8 presents the macrostructure of the welded joint observed on the cross-section of the weld axis. The joint has a regular symmetrical shape with visible underfilling of the weld face, without visible pores.

Figure 9 and 10 shows the microstructure of base materials: 2024 T351 aluminum alloy and 6082 T6 aluminum alloy. Elongated grains in the rolling direction were observed on the sample of 2024-T351 alloy. SEM/EDS analysis identified coarse intermetallic particles Al-Cu-Fe-Mn-Si (>10 μm), finer Al-Cu-Mg, Al-Cu-Mn, Al-Cu-Mg-Si and Al-Si-Cu-Mg (Figure 11). The fine particles can be precipitates of alloys elements, Al-Cu and Al-Cu-Mg based.

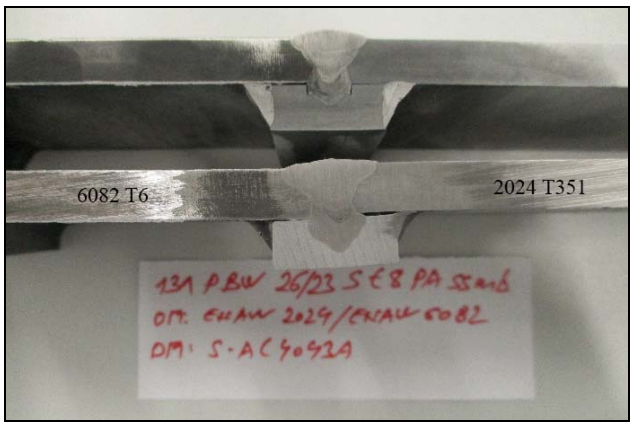

Figure 8. Macrostructure of a welded joint made with a backing material.

Microstructure of base metal – aluminum alloy 6082-T6, also consists of a wide range of intermetallic phases (IMP) formed during processing.

Larger particles in the direction of rolling Al-Fe-Mn-Mg-Si-Cr, Al-Mg-Si-Mn, Al-Mg-Si (Figure 12), and fine precipitate particles Mg-Si, formed during the artificial aging process were observed.

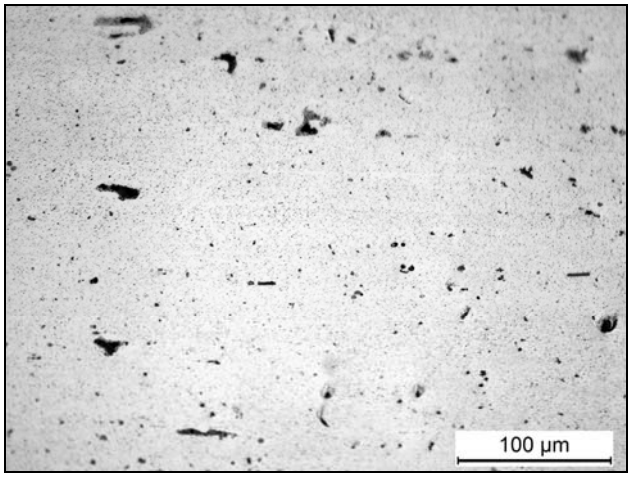

Figure 9. Distribution of second phase particles in 2024 T351 aluminum alloy. (LM).

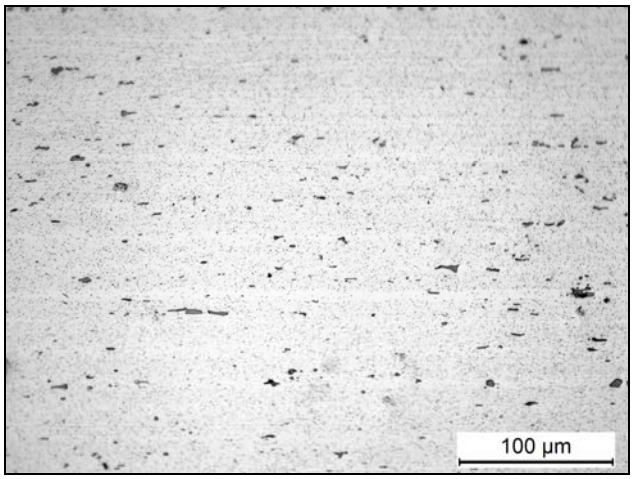

Figure 10. Distribution of second phase particles in 6082 T6 aluminum alloy. (LM).

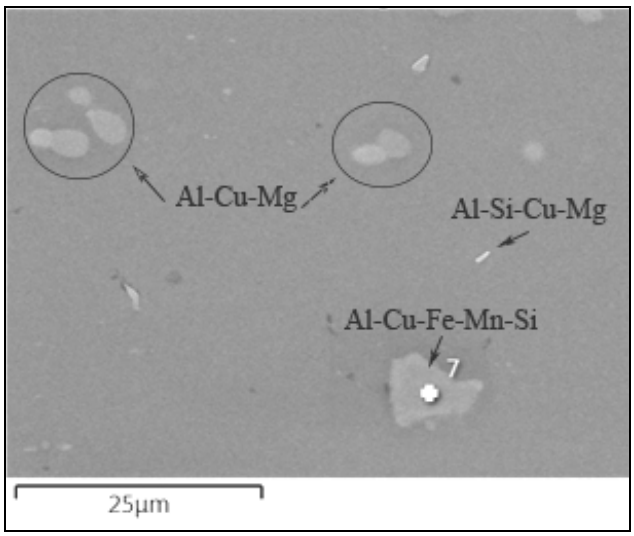

Figure 11. Second phase particles in 2024-T351 alloy. (SEM).

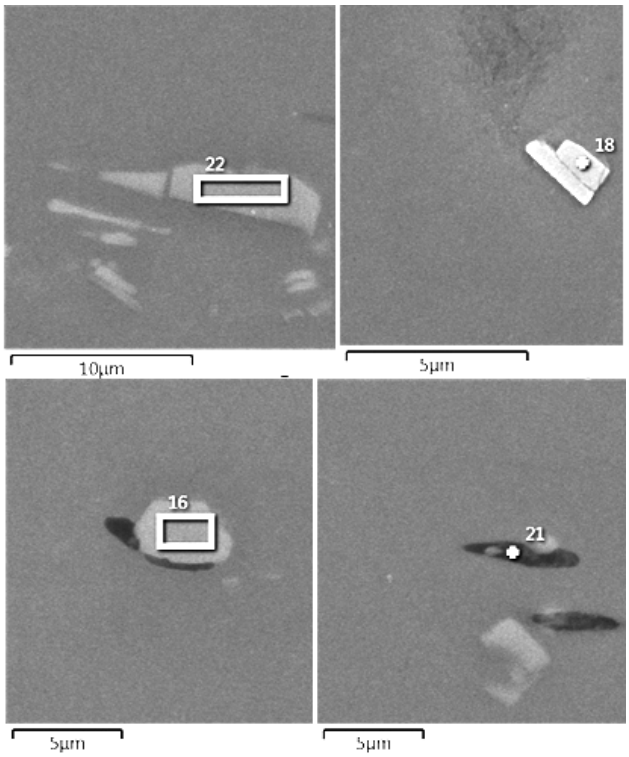

Figure 12. Second phase particles in 6082-T6 alloy. Al-Fe-Mn-Mg-Si-Cr, Al-Si-Mg, Al-Mg-Si-Mn, Al-Mg-Si,. (SEM).

Figure 13 shows the microstructure of the heat affected zone (HAZ) between the weld metal (WM) and the 2024-T351 base metal. Lower density of the precipitates in the HAZ was observed.

Figure 14 shows the microstructure of the HAZ between the weld metal and the 6082-T6 base metal. A narrow zone of columnar crystals is present in the WM to the HAZ. The precipitates are formed along the grain boundaries and within the grains in coarse form. The precipitates in the HAZ distributed randomly as globular coarse particles, as well as, lower density of the fine precipitates in the HAZ was observed.

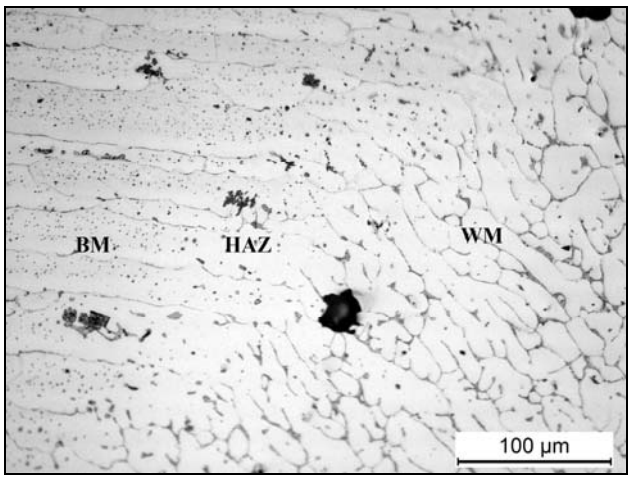

Figure 13. Heat affected zone in 2024 T351 alloy. (LM).

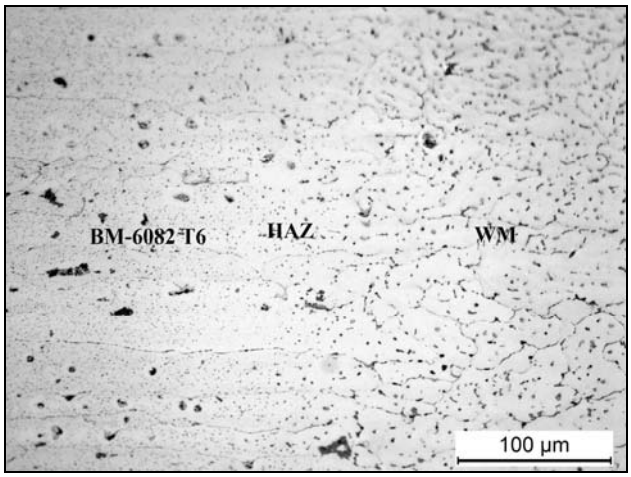

Figure 14. Heat affected zone in 6082 T6. (LM).

Figure 15 shows the microstructure of weld metal (WM) MIG joints for dissimilar aluminum alloys (2024-T351 and 6082-T6).

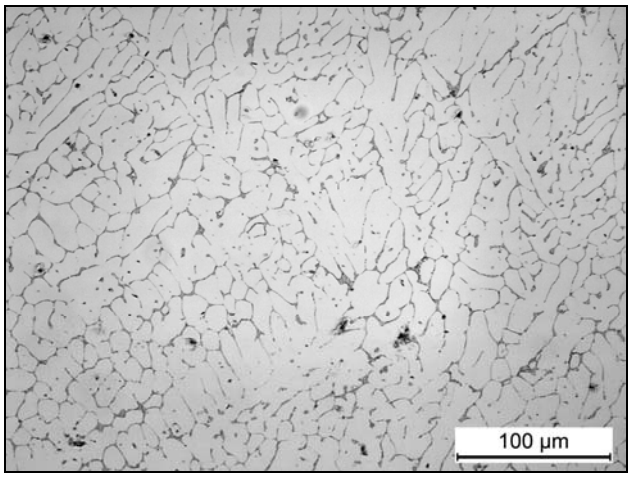

Figure 15. Microstructure of the weld metal. (LM).

4. DISCUSSION

The microstructure of the weld metal obtained by the MIG welding process is significantly different from the microstructure of the base metals, and accordingly, the

mechanical properties of the welded joint are lower than the mechanical properties of the base metals. A lower ductility was also observed during the tensile test.

The fracture location of specimen for tensile testing is in base metal – 6082-T6. The results of bending tests indicate poor technological properties of welded joints. A small bending angle until the appearance of a crack indicates that the welded joints are very brittle according to [8-11].

The hardness of the weld metal, measured near the weld face and near the weld root, is about 80 HV, which is less than the softer base metal 6082-T6, which has a hardness of about 90 HV, and significantly less than the base metal 2024-T351, which has a hardness of about 150 HV. The hardness of HAZ towards 6082-T6 is about 60 HV, lower than in the weld metal zone. HAZ towards 2024-T351 has a hardness of about 120 HV, but, also lower compared to 2024 base metal. Such hardness distribution (Figure 7) is obtain due to microstructural changes in HAZs in age-hardenable alloys (Figures 11 and 12). When the alloy is exposed to thermal cycle during welding, the hardening fine precipitates (dispersoids) dissolve, and at the same time the others overage. There is more coarse particles with decreasing amount of small dispersoids. Decrease density of smallest dispersoids lead to reduction of hardness/strength [12, 13].

The heat input of joins, the base metals and the filler metal create a zone of weld metal with a structure that is different from the structure of the base metals. A higher percentage of silicon (about 5%) in the filler material is useful for increasing the ductility of the welded structure and another benefits are low hot cracking sensitivity in most applications, excellent corrosion resistance, and low shrinkage rate/reduced distortion [14]. The melting zone, or weld metal area, is created by filling a previously prepared groove with molten filler material. After solidification, the weld metal has a characteristic casting structure (Figure 13). The layer that hardens last has a distinctly dendritic structure, which is characterized by the appearance of liquation, i.e. local chemical inhomogeneity, due to the lack of time for the diffusion of atoms of alloying elements. The grains are of different sizes and have a directional orientation [8].

5. CONCLUSION

Based on the above, it can be concluded:

- The tensile strength of the welded joint is (198 MPa) compared to (310 MPa) alloy 6082-T6 which is a weaker welded joint material, i.e. the reduction in strength is about (36%).
- The fracture of the tensile test specimen was found to occur on the 6082-T6 aluminum alloy side.
- Weld metal hardness is 55% lower than base metal hardness 2024-T351.
- To improve the performance of welded joints of different aluminum alloys 2024-T351 and 6082-T6, optimal welding parameters must be selected.

ACKNOWLEDGMENTS

This research work was financially supported by the Ministry of Education, Science and Technological Development of the Republic of Serbia (Contracts No. 451-03-68/2022-14/200109 and 451-03-68/2022-14/200325). This paper is the result of research within the bilateral project with the Republic of Slovenia "Providing high reliability of aluminum structures and their parts in transport technics" in the project cycle 2020-2022 (project no. 337-00-21/2020-09/48).

References

[1] Metals Handbook, Vol. 6: *Welding, Brazing and Soldering*, ASM Metals Park, Ohio, 1997.

[2] Molian, P. A., Srivatsan, T. S.: *Weldability of aluminium-lithium alloy 2090 using laser welding*, J. Mater. Sci., 25(7) (1990) 3347–3358.

[3] Heinz, A., Haszler, A., Keidel, C., Moldenhauer, S., Benedictus, R. Miller, W.: *Recent development in aluminium alloys for aerospace applications*, Mater. Sci. Eng. A, 280 (2000) 1, pp.102–107.

[4] Milcic, M., Vuherer, T., Radisavljevic, I., Milcic, D.: *Experimental Investigation of Mechanical Properties on Friction Stir Welded Aluminum 2024 Alloy*, Springer Nature Switzerland AG 2019, N. Mitrovic et al. (Eds.): CNNTech 2018, LNNS 54, pp. 44-58.

[5] Milcic, M., Vuherer, T., Radisavljevic, I., Milcic, D., Kramberger, J.: *The influence of process parameters on the mechanical properties of friction stir welded joints of 2024 T351 aluminum alloys*, Materials and technology 53(6) (2019) 771–776.

[6] ASM Handbook, Vol.2 - *Properties and Selection: Nonferrous Alloys and Special-Purpose Materials*, Edition Metals Handbook, ASM International 10th Ed. 1990.

[7] ASTM E8M -Standard Test Methods for Tension Testing of Metallic Materials,

[8] Nawres, N., J.: *Mechanical Properties of MIG Joints for Dissimilar Aluminum Alloys (2024-T351 and 6061-T651)*, Al-Khwarizmi Engineering Journal, 12(3) (2016) 121- 128.

[9] Cavaliere, P., Nobile, R., Panella, F. W., Squillace, A.: *Mechanical and microstructural behavior of 2024-7075aluminum alloy sheets joined by friction stir welding*, International Journal of Machine Tools and Manufacture 46 (2005) 588-594.

[10] Muafaq, M. S.: *Studying the effect of joint design, angle and heat treatment on mechanical properties of the aluminum alloy weldments (7020-T6) by MIG process*, Master Thesis, Technical College/Baghdad, 2005.

[11] Missori, S., Sili, A.: *Mechanical behavior of 6082-T6 aluminum alloy welds*, Metallurgical Science and Technology, 18 (2000) 12-18.

[12] Rakhmonov, J. et al. *Improving the Mechanical Response of Al–Mg–Si 6082 Structural Alloys during High-Temperature Exposure through Dispersoid Strengthening,* Materials 2020, 13, 5295.

*[13]*Fang, X. at al., *Precipitation sequence of an aged Al-Mg-si Alloy, J. Min. Metall. Sect. B-Metall. 46 (2) B (2010) 171 – 180.*

[14] AMS 4190K Alloy 4043, https://weldingwarehouseinc.com